Oncology Research, Vol. 28, pp. 161–175
Printed in the USA.

0965-0407/20 $90.00 + .00
DOI: https://doi.org/10.3727/096504019X15736439848765
E-ISSN 1555-3906
www.cognizantcommunication.com

Enhancement of Radiosensitivity by Eurycomalactone in Human NSCLC Cells Through G_2/M Cell Cycle Arrest and Delayed DNA Double-Strand Break Repair

Nahathai Dukaew,*† Teruaki Konishi,‡§ Kongthawat Chairatvit,¶ Narongchai Autsavapromporn,# Noppamas Soonthornchareonnon,** and Ariyaphong Wongnoppavich†

*Graduate/PhD's Degree Program in Biochemistry, Faculty of Medicine, Chiang Mai University, Chiang Mai, Thailand
†Department of Biochemistry, Faculty of Medicine, Chiang Mai University, Chiang Mai, Thailand
‡Single Cell Radiation Biology Group, Institute for Quantum Life Science, National Institutes for Quantum and Radiological Science and Technology (QST), Chiba, Japan
§Department of Basic Medical Sciences for Radiation Damages, National Institute of Radiological Sciences (NIRS), Chiba, Japan
¶Department of Oral Biology, Faculty of Dentistry, Mahidol University, Bangkok, Thailand
#Division of Radiation Oncology, Department of Radiology, Faculty of Medicine, Chiang Mai University, Chiang Mai, Thailand
**Department of Pharmacognosy, Faculty of Pharmacy, Mahidol University, Bangkok, Thailand

Radiotherapy (RT) is an important treatment for non-small cell lung cancer (NSCLC). However, the major obstacles to successful RT include the low radiosensitivity of cancer cells and the restricted radiation dose, which is given without damaging normal tissues. Therefore, the sensitizer that increases RT efficacy without dose escalation will be beneficial for NSCLC treatment. Eurycomalactone (ECL), an active quassinoid isolated from *Eurycoma longifolia* Jack, has been demonstrated to possess anticancer activity. In this study, we aimed to investigate the effect of ECL on sensitizing NSCLC cells to X-radiation (X-ray) as well as the underlying mechanisms. The results showed that ECL exhibited selective cytotoxicity against the NSCLC cells A549 and COR-L23 compared to the normal lung fibroblast. Clonogenic survival results indicated that ECL treatment prior to irradiation synergistically decreased the A549 and COR-L23 colony number. ECL treatment reduced the expression of cyclin B1 and CDK1/2 leading to induce cell cycle arrest at the radiosensitive G_2/M phase. Moreover, ECL markedly delayed the repair of radiation-induced DNA double-strand breaks (DSBs). In A549 cells, pretreatment with ECL not only delayed the resolving of radiation-induced -H2AX foci but also blocked the formation of 53BP1 foci at the DSB sites. In addition, ECL pretreatment attenuated the expression of DNA repair proteins Ku-80 and KDM4D in both NSCLC cells. Consequently, these effects led to an increase in apoptosis in irradiated cells. Thus, ECL radiosensitized the NSCLC cells to X-ray via G_2/M arrest induction and delayed the repair of X-ray-induced DSBs. This study offers a great potential for ECL as an alternative safer radiosensitizer for increasing the RT efficiency against NSCLC.

Key words: Eurycomalactone; Radiosensitization; Non-small cell lung cancer (NSCLC); G_2/M arrest; DNA double strand break (DSB) repair

INTRODUCTION

Lung cancer is the most common cancer and the leading cause of cancer mortality worldwide[1]. Non-small cell lung cancer (NSCLC) accounts for 85% of all lung cancer cases, with adenocarcinoma, squamous cell carcinoma, and large cell carcinoma representing the three major histological subtypes[2]. Radiotherapy (RT) using ionizing radiation, especially X-radiation (X-ray), is an important treatment option and widely accepted for localized NSCLC. Yet the low radiation sensitivity of lung cancer cells turns out to be the major obstacle to RT efficacy. Moreover, the radiation dose delivered to the targeted tumor cannot be escalated due to surrounding normal tissue damage. Consequently, the average 5-year survival rate of NSCLC patients after treatment is still low and has not significantly improved in recent decades[3].

Several factors that are related to the cancer radiation sensitivity can be a promising target for radiosensitizers

Address correspondence to Ariyaphong Wongnoppavich, Department of Biochemistry, Faculty of Medicine, Chiang Mai University, 110 Intravaroros Rd., Sripoom, Muang Chiang Mai 50200, Thailand. Tel: +66-5393-4436, ext. 216; Fax: +66-53894-031; E-mail: ariyaphong.w@cmu.ac.th

such as the capacity to repair the radiation-induced DNA damages[4] and the redistribution of cell cycle phase[5]. Inhibition of the DNA double-strand break (DSB) repair cascade has been reported for various plant phytochemicals such as mangiferin[6] and genistein[7] to significantly enhance the radiosensitivity of cancer cells to ionizing radiation. Furthermore, the induction of radiosensitive G_2/M cell cycle arrest leading to apoptosis has been successful for cancer radiosensitization by several plant-derived compounds such as genistein[8] and gingerol[9]. Thus, a phytochemical radiosensitizer may be potentially beneficial for NSCLC treatment to improve the therapeutic efficacy of lung cancer cell mortality without dose escalation and significant collateral damage to neighboring normal tissues.

Eurycoma longifolia Jack is a popular herbal folk medicine of Southeast Asian countries. It is well known as "tongkat ali" (Malaysian ginseng) or "Rak Pla Lai Pueak" in Thailand. The root and rhizome have long been traditionally used to alleviate various diseases including malaria, sexual insufficiency, and cancer[10]. Moreover, the cytotoxic potential of this plant against lung cancer cells has been previously demonstrated[11]. The in vitro anticancer activity of many quassinoids, the main bioactive compounds derived from *E. longifolia*, has been established[12,13]. Interestingly, among all isolated quassinoids from *E. longifolia*, a C-19 quassinoid called eurycomalactone (ECL) (Fig. 1A) was found to have the most potent cytotoxicity against various cancer cell types including human lung cancer cells[12, 13]. In this study, we aimed to investigate the anticancer and radiosensitizing potentials of ECL on NSCLC cells. In addition, we further elucidated possible underlying mechanisms by which ECL enhances the efficacy of X-ray irradiation to NSCLC through alteration of cell cycle redistribution and DNA repair pathway.

MATERIALS AND METHODS

Isolation of ECL From E. longifolia *Jack*

Roots of *E. longifolia* Jack were collected from Betong, Yala, Thailand. Authentication was carried out at the herbarium of the Royal Forest Department, Ministry of Agriculture and Cooperatives, Bangkok, Thailand. The voucher numbers were deposited at the Department of Pharmaceutical Botany, Faculty of Pharmacy, Mahidol University (CHUAKUL 03558). ECL was isolated as previously described with a minor adjustment[13]. Briefly, miniaturized dried roots of *E. longifolia* Jack (4.8 kg) were macerated thoroughly with

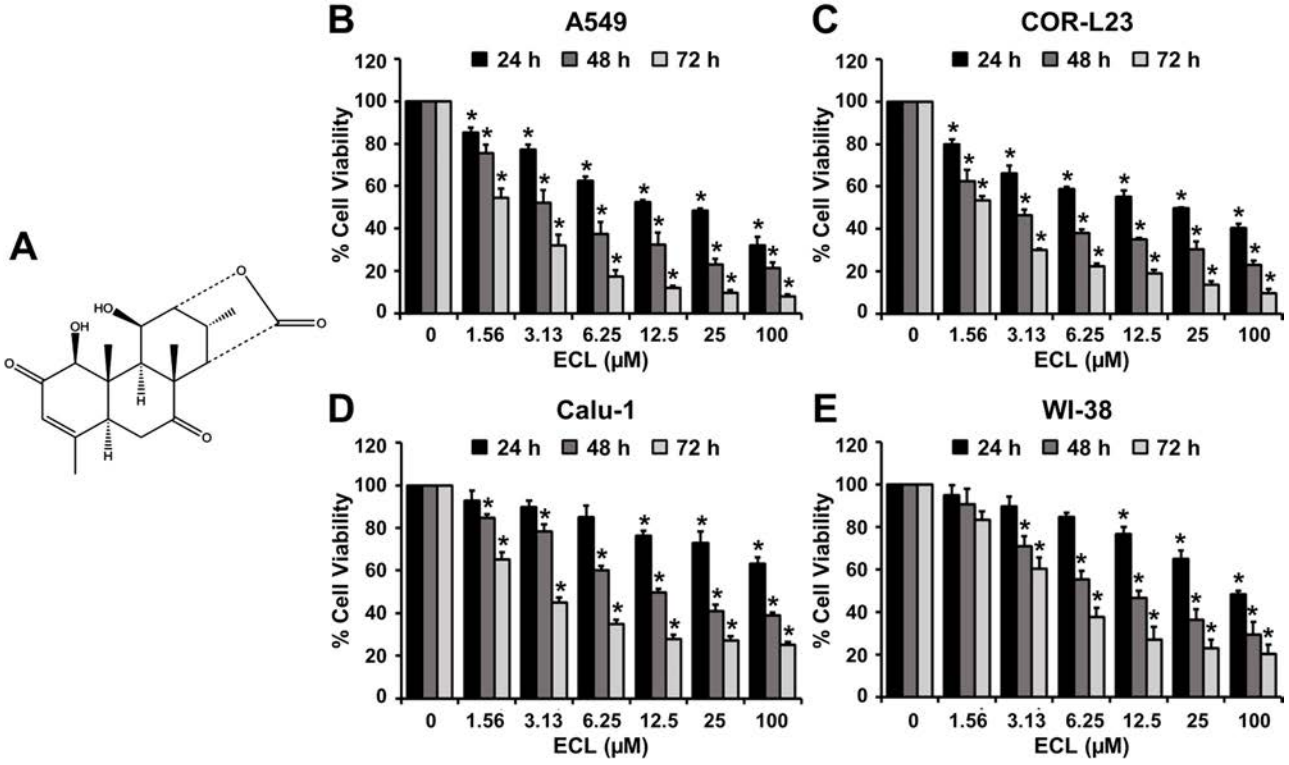

Figure 1. Cytotoxic effects of eurycomalactone (ECL) on human lung cell lines. (A) Chemical structure of ECL. The cell viability percentage of A549 (B), COR-L23 (C), Calu-1 (D), and WI-38 cells (E) that were grown in the presence of ECL (0–100 μM) at 24, 48, or 72 h. All data are presented as mean ± SD. $n = 3$. *$p < 0.001$ versus control at equal incubation periods.

ethanol. The ethanolic fraction was then evaporated to yield 220 g of crude ethanolic extract (F1). The F1 was separated using a solvent partition between CH_2Cl_2 (F2, 34.8 g) and water (F3). The CH_2Cl_2 part was further fractionated by column chromatography using silica gel 60 (70–230 mesh ASTM; Merck KGaA, Darmstadt, Germany) as an adsorbent. A gradient mixture of CH_2Cl_2 and Me_2CO was used as mobile phase providing 12 fractions (Fr201–Fr212). Fraction 204 was then rechromatographed on a silica gel column eluted with a gradient mixture of n-hexane, CH_2Cl_2, and Me_2CO to yield fractions DF1–DF15. A preparative thin-layer chromatography C-18 RP (Merck) using a mixture of water, acetonitrile, and methanol as a mobile phase together with recrystallization process was applied to purify ECL (20 mg) from fraction DF9. The ECL detection was performed by HPLC and MS analyses.

Cell Lines and Cell Culture

Human lung adenocarcinoma A549 (RCB0098) and human normal lung fibroblast WI-38 cells (RCB0702) were obtained from the RIKEN Bioresource Center, Ibaraki, Japan. Human lung epidermoid carcinoma Calu-1 was purchased from the Cell Lines Service (CLS; Eppelheim, Germany) and human lung large cell carcinoma COR-L23 from the European Collection of Authenticated Cell Cultures (ECACC; Salisbury, UK). A549 and WI-38 cells were cultured in D-MEM medium (Gibco; Thermo Fisher Scientific, Inc., Waltham, MA, USA). Calu-1 and COR-L23 were cultured in RPMI-1640 medium (Gibco). These culture media were supplemented with 10% (v/v) fetal bovine serum (FBS; Hyclone; GE Healthcare Life Sciences, Logan, UT, USA) and 1% antibiotics (Gibco) at 37°C in a 5% CO_2 humidified atmosphere. All of the cell lines are mycoplasma free. The continuous cell lines are routinely checked in every other month by a PCR method using a service from The Center for Veterinary Diagnosis, Faculty of Veterinary Science, Mahidol University Salaya Campus, Nakorn Pathom, Thailand.

MTT Assay

The cells were seeded in a 96-well plate for 24 h and treated with various concentrations of ECL for 24, 48, or 72 h. Subsequently, the number of viable cells was determined by the MTT (3-[4,5-methylthiazol-2-yl]-2,5-diphenyl-tetrazolium bromide) assay as described previously[14]. Finally, the absorbance (OD) was read at 540/630 nm using a microplate reader (Bio-Rad Laboratories, Inc., Hercules, CA, USA). The cell survival was expressed as cell viability = $(OD_{treated}/OD_{control}) \times 100\%$.

X-Ray Irradiation

The cells were irradiated using an X-ray generator (TITAN; Shimazu Corporation, Kyoto, Japan), which was set at 200 kVp and 20 mA, and the irradiation was made through a copper and aluminum filter with a thickness of 0.5 mm, producing an effective energy of approximately 83 keV. The dishes holding the cells were placed at a distance of 500 mm from the X-ray target, which received X-ray doses at a dose rate of about 1 Gy/min.

Clonogenic Cell Survival Assay

Cells were pretreated with or without ECL at IC_{20} and IC_{50} for 24 h, followed by X-irradiation at 0, 1, 2, 3, 5, or 7 Gy. The cells were reseeded, and culture was continued for 14 days, then fixed with 3% paraformaldehyde, and stained with crystal violet. Colonies containing more than 50 cells were counted to calculate the plating efficiency (PE); the ratio of the number of colonies to the number of cells seeded in the nonirradiated group and the survival fraction (SF); the mean number of colonies divided by (the number of cells seeded × PE). Survival curve data were fit with a linear-quadratic (LQ) model using the KaleidaGraph program (Synergy Software, Reading, PA, USA).

Immunofluorescence

A549 cells in four-well chamber slides were pretreated with or without ECL for 24 h and followed by X-irradiation (2 Gy). Postirradiation was done at 1, 4, or 24 h, and the -H2AX and 53BP1 foci were detected using the immunofluorescence assay previously described[15]. The following primary and secondary antibodies were used: anti- -H2AX (Ser139; No. 05-636; Merck), anti-53BP1 (H-300; No. sc-22760; Santa Cruz Biotechnology, Inc., Santa Cruz, CA, USA), goat anti-mouse IgG secondary antibody (Alexa 488; No. A11001; Invitrogen, Life Technologies, Carlsbad, CA, USA), and goat anti-rabbit IgG secondary antibody (Alexa 594; No. A11037; Invitrogen, Life Technologies). Nuclei were counterstained with Hoechst 33342 (Invitrogen, Life Technologies). Fluorescent images were obtained by fluorescence microscopy (SPICE-offline microscope system; NIRS, Chiba, Japan). The averaged -H2AX fluorescence intensities per nucleus were analyzed by ImageJ software [National Institutes of Health (NIH), Bethesda, MD, USA].

Flow Cytometric Analysis of Cell Cycle

After the desired times of ECL pretreatment, cells were irradiated with X-rays and further incubated for 24 h. Cells were then collected, fixed gently in 70% ethanol, and stored at −20°C overnight. The fixed cells were stained with Muse® Cell Cycle Kit (EMD Millipore Corp., Billerica MA, USA) for 30 min at room temperature in the dark. The cell cycle phase distributions were determined by Muse® Cell Analyzer (EMD Millipore Corp.) using the Cell Cycle software module. The cell cycle phases sub-G_1, G_1, S, and G_2/M were analyzed with GuavaSoft 2.7 software (EMD Millipore Corp.).

Flow Cytometric Analysis of Apoptosis

After exposure to ECL for 24 h, A549 cells were X-ray irradiated with 2 Gy and further incubated for 24 h. Apoptosis was quantified by staining with Muse® Annexin-V and Dead Cell Kit (EMD Millipore Corp.) according to the manufacturer's instructions. The quantitative analysis of live, early, and late apoptosis and cell death were obtained by the Muse® Cell Analyzer (EMD Millipore Corp.) using the Annexin-V and Dead Cell software module.

Western Blotting Analysis

Western blot analysis was performed as described previously[16] using corresponding antibodies against cyclin B1 (No. sc-245, Santa Cruz Biotechnology, Inc.), cyclin-dependent kinase 1/2 (CDK1/2; No. sc-53219, Santa Cruz Biotechnology, Inc.), KDM4D (No. ab93694, Abcam, Cambridge, UK), Ku-80 (No. C48E7, Cell Signaling Technology, Inc., Denver, CO, USA), and the internal control, -actin (No. A2066, Sigma-Aldrich). Protein bands were visualized via chemiluminescence using horseradish peroxidase-conjugated goat anti-rabbit (No. 1706515) or goat anti-mouse (No. 1706516) immunoglobulin G (Bio-Rad Laboratories). The normalized mean density of immunocrossreactive band was quantified by ImageJ software (NIH) and expressed as the ratio of density between the protein and -actin relative to the control group.

Reverse Transcription-Quantitative Polymerase Chain Reaction (RT-qPCR)

Total RNA was extracted using TRIzol reagent (Invitrogen, Life Technologies), and cDNA was generated using 1 µg of total RNA with oligo dT (deoxythymidine) primers and RevertAid reverse transcriptase (Thermo Scientific, New York, NY, USA). The target cDNA was amplified using specific primers with SensiFAST™ SYBR® Lo-ROX Kit (Bioline Ltd., London, UK). The oligonucleotide primers were obtained from Bio Basic Inc (Toronto, ON, Canada). The primer sequences for cyclin B1 (CCNB1) were 5 -ATGTGCCCCTGCAGAAGAAG-3 (forward) and 5 -TTTCCAGTGACTTCCCGACC-3 (reverse); for CDK1 were 5 -CGCGGAATAATAAGCCGGGA-3 (forward) and 5 -CATGGCTACCACTTGACCTGT-3 (reverse); for lysine demethylase 4D (KDM4D) were 5 -GGATGGGGCTTTGATGGACA-3 (forward) and 5'-AAGACAGCCCGTGGACTTAG-3 (reverse); for Ku-80 (XRCC5) were 5 -TGTGCTGTGTATGGACGT GG-3 (forward) and 5 -CTGATCCCCACCAGAAAG GG-3 (reverse); and for GAPDH were 5 -GAGCCAA AAGGGTCATCATC-3 (forward) and 5 -TAAGCAGT TGGTGGTGCAGG-3 (reverse). The expression level of each target gene was normalized to GAPDH and analyzed using the comparative threshold (C_t) method (7500 software v2.0.5; Applied Biosystem, Thermo Fisher Scientific Inc., Foster City, CA, USA). Quantitative assays were calculated based on the following equation: relative quantitation (RQ) = $2^{-\ Ct}$.

Statistical Analysis

Significant differences between all data were analyzed and compared by one-way analysis of variance (ANOVA) using the SPSS 22.0 software (SPSS Inc., Chicago, IL, USA). Differences with a value of $p < 0.05$ are considered statistically significant.

RESULTS

ECL Selectively Inhibited the Viability of A549 and COR-L23 NSCLC Cells

The dose- and time-dependent cytotoxic effects of ECL were examined using MTT assay in human NSCLC cell lines, namely, A549 (adenocarcinoma), Calu-1 (squamous cell carcinoma), and COR-L23 (large cell carcinoma) versus the normal human lung fibroblast cell line WI-38. As shown in Figure 1B–E, ECL significantly decreased the viability of all tested cell lines in dose- and time-dependent manners. The ECL concentrations required for 20% and 50% inhibition of cell viability (IC_{20} and IC_{50}) and the selectivity index (SI) of ECL for anticancer therapy at 24, 48, and 72 h were calculated as shown in Tables 1 and 2. Noticeably, ECL exerted great selective cytotoxic activity against A549 and COR-L23 cells, with the highest SI observed at 24 h (SI = 4.59 and 3.70, respectively) but not on Calu-1 cells, compared to the normal lung fibroblast WI-38. In all following experiments, A549 and COR-L23 cells were selected to study the radiosensitizing effect of ECL at noncytotoxic dose (IC_{20} = 2.5 and 1.5 µM, respectively) and cytotoxic dose of 24 h (IC_{50} = 20 and 25 µM, respectively).

ECL Synergistically Sensitized the Radiosensitivity of NSCLC Cells to X-Radiation

The radiosensitizing potential of ECL on A549 and COR-L23 cells was determined using the clonogenic survival assay. As shown in Figure 2A and C, pretreatment with ECL for 24 h before X-ray treatment significantly reduced the clonogenic survival of both NSCLC cells compared to irradiation treatment alone ($p < 0.05$). Moreover, the sensitization ratio depended on the doses of both radiation and ECL (Fig. 2B and D). The degree of radiosensitization was quantified from the survival curves by comparing the radiation doses at 10% surviving fraction (D_{10}) and calculating the sensitizer enhancement ratio at 10% surviving fraction (SER_{10}), with an SER_{10} value >1 indicating an enhancement of radiosensitivity. From the results, the combination treatment with IC_{20} and IC_{50} of ECL significantly decreased the dose of radiation that was used to reach 10% surviving fraction (D_{10}) of both A549 and COR-L23 cells with the SER_{10}

Table 1. Cytotoxic Effect of Eurycomalactone (ECL) Against Three Different Non-Small Cell Lung Cancer (NSCLC) Cells (A549, COR-L23, and Calu-1) and Normal Lung Fibroblasts (WI-38)

	IC_{20} (μM)				IC_{50} (μM)			
Time	A549	COR-L23	Calu-1	WI-38	A549	COR-L23	Calu-1	WI-38
24 h	2.57 ± 0.44*	1.57 ± 0.17**	9.21 ± 1.25	8.63 ± 3.14	20.17 ± 2.69**	25.02 ± 1.00**	>100	92.51 ± 6.95
48 h	1.30 ± 0.23	0.84 ± 0.11	2.82 ± 0.60	2.37 ± 0.51	3.77 ± 0.93 *	2.74 ± 0.34*	12.76 ± 1.91	9.88 ± 1.69
72 h	0.69 ± 0.06	0.67 ± 0.03	0.90 ± 0.09	1.76 ± 0.23	1.90 ± 0.28	1.80 ± 0.11	2.73 ± 0.21	4.51 ± 0.70

IC_{20} and IC_{50} are the concentrations required for 20% and 50% inhibition of cell viability, respectively. The values (μM) are expressed as mean ± SD of three independent experiments.
*$p < 0.05$, **$p < 0.01$ versus the normal lung fibroblast WI-38 at equal incubation periods.

Table 2. Selectivity Index (SI) of ECL Against Three Different NSCLC Cells (A549, COR-L23, and Calu-1) Compared to the Normal Lung Fibroblast (WI-38)

Treatment Time	A549	COR-L23	Calu-1
24 h	4.59	3.70	<0.93
48 h	2.62	3.61	0.77
72 h	2.37	2.51	1.65

Selectivity index (SI) = IC_{50} of ECL in a normal cell line (WI-38)/IC_{50} of the ECL in cancer cell line (NSCLC cells).

values >1 compared to X-ray irradiation alone (Table 3). Thus, the radiation dose could be reduced when combined with ECL, but still showed similar inhibitory effect to the higher dose of irradiation alone. These results suggest that ECL synergistically sensitizes the effect of radiation-induced loss of clonogenic potential in NSCLC cells.

ECL Induced Cell Cycle Arrest at the Radiosensitive G_2/M Phase and Induced Apoptosis in Irradiated NSCLC Cells

Cancer cells are most sensitive to radiation during the G_2/M phase of the cell cycle[5]. We determined the cell cycle distribution in A549 and COR-L23 cells to gain further insight into the radiosensitization mechanism of ECL. As shown in Figure 3, after treatment with IC_{20} or IC_{50} (μM) of ECL alone, the percentage of A549 and COR-l23 cells in the G_2/M phase was significantly higher than that of untreated control cells. Interestingly, the percentage of both NSCLC cells in the G_2/M phase after combined treatment with IC_{20} or IC_{50} (μM) of ECL and X-ray was significantly increased when compared to the X-ray treatment alone. In addition, the combination treatment of ECL not only induced G_2/M arrest in irradiated cells but also significantly increased the sub-G_1 population, which is regarded as apoptotic cells. The apoptosis induction induced by the combination treatment was confirmed in both NSCLC cell lines by the Annexin-V–FITC/PI staining assay using flow cytometry (Fig. 4A–D). These results confirmed that ECL enhances the effect of radiation on cancer cell killing.

ECL Downregulated the Key G_2/M Regulatory Proteins in Irradiated NSCLC Cells

Because ECL arrested the cells in the G_2/M phase, we next assessed the effect of ECL alone or in combination with X-ray on the expression of protein and mRNA of key G_2/M regulatory molecules, cyclin B1 and CDK1/2. ECL treatment alone could downregulate the expression of both G_2/M regulatory proteins in a dose-dependent manner. Importantly, compared to the X-ray treatment alone, the

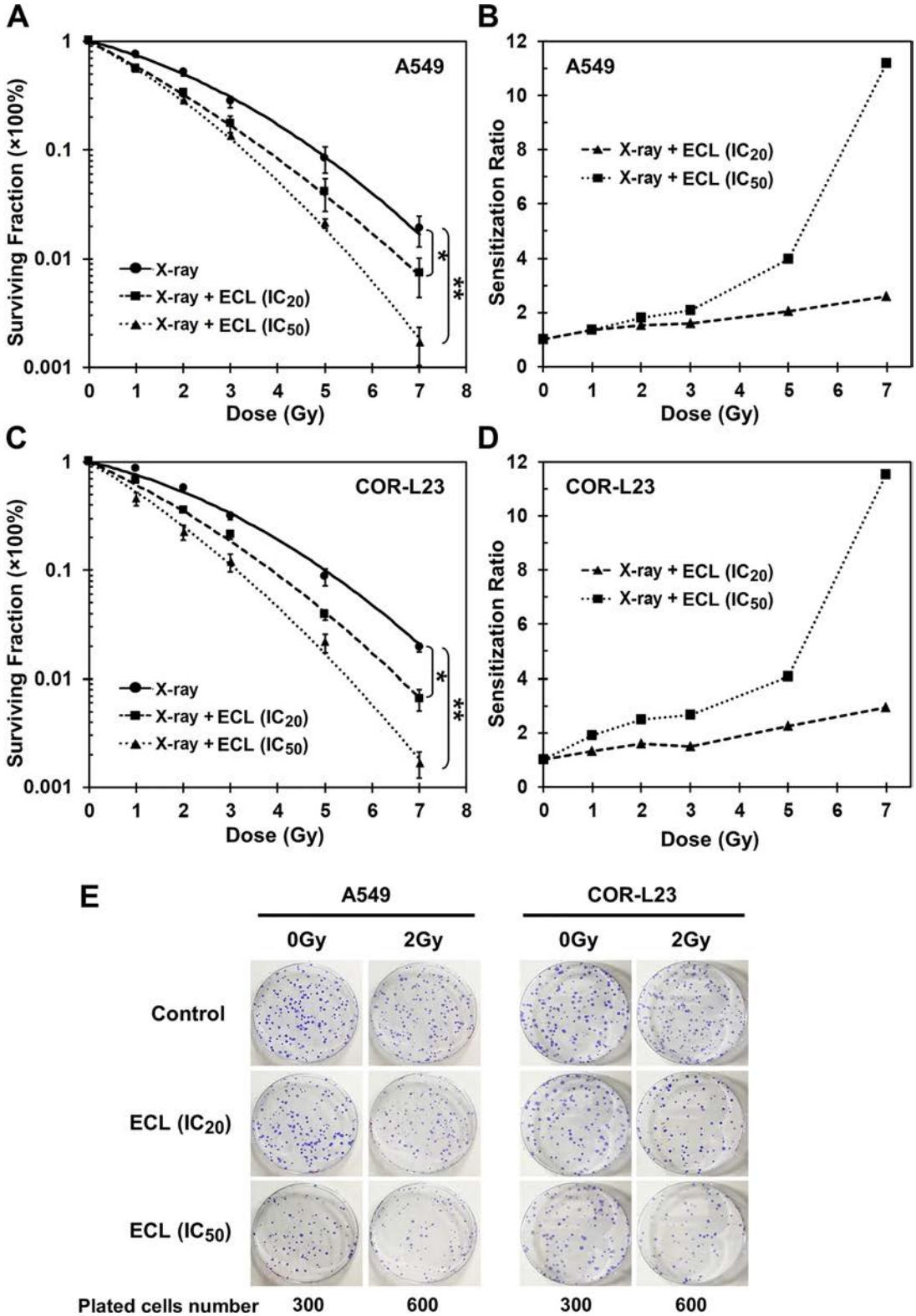

Figure 2. Radiosensitizing efficiency of ECL on A549 and COR-L23 NSCLC cells by a clonogenic survival assay. The clonogenic survival curve represented the radiosensitivity of A549 (A) and COR-L23 cells (C) treated with varying doses of X-radiation alone or in combination with IC_{20} or IC_{50} concentrations of ECL. The radiosensitization ratio of ECL on A549 (B) and COR-L23 (D) cells obtained from the survival curve. (E) Representative pictures of colonies. All data are presented as mean ± SD. $n = 3$. *$p < 0.05$, **$p < 0.01$ versus X-ray treated alone group.

Table 3. The Radiobiological Parameters of the NSCLC Cells Treated With or Without ECL Before Irradiation

	A549			COR-L23		
	X-Ray	X-Ray + ECL (IC_{20})	X-Ray + ECL (IC_{50})	X-Ray	X-Ray + ECL (IC_{20})	X-Ray + ECL (IC_{50})
SF2	0.51 ± 0.06	0.28 ± 0.05	0.19 ± 0.03	0.56 ± 0.01	0.36 ± 0.03	0.23 ± 0.04
D_{10}	4.45 ± 0.67	3.60 ± 0.52	3.31 ± 0.20	4.90 ± 0.14	3.81 ± 0.09	3.22 ± 0.13
SER_{10}	1.00 ± 0.00	1.24 ± 0.02	1.34 ± 0.14	1.00 ± 0.00	1.29 ± 0.01	1.52 ± 0.10

SF2, survival fraction at 2Gy; D_{10}, the dose required to obtain a survival level of 10%; SER_{10}, sensitizer enhancement ratio at 10% surviving fraction. Values were calculated with linear-quadratic model and presented as mean ± SD of three independent experiments.

level of these proteins after combined treatment with IC_{20} or IC_{50} (μM) of ECL and X-ray was significantly suppressed compared to the X-ray treatment alone in both A549 (Fig. 5A–C) and COR-L23 cells (Fig. 5D–F). However, ECL treatment alone or combined with X-ray did not influence the mRNA expression of cyclin B1 and CDK1/2 (Fig. 5G and H). Accordingly, the decreased expression of these G_2/M regulatory proteins could lead to the G_2/M arrest induction.

ECL Suppressed the Repair of Radiation-Induced DNA Double-Strand Breaks

The capacity for repair of DNA double-strand breaks (DSBs) becomes one of the most important factors for cancer cell resistance to radiation therapy[17]. A549 cells were pretreated with 2.5 or 20 μM ECL for 24 h followed by irradiation. Foci of phosphorylated histone H2A family member X (-H2AX), which is a biomarker for DSBs, were then detected (Fig. 6A). The total -H2AX fluorescent levels per nucleus at various time points (1, 4, and 24 h) of postirradiation were also quantitatively measured to observe the DSB repair kinetics of A549 cells (Fig. 6B). Compared to untreated control cells, treatment with ECL at both concentrations presented few or no -H2AX foci, which implied that ECL alone does not significantly induce DSBs. Exposure of A549 cells with 2 Gy radiation alone significantly increased the level of -H2AX 3.6-fold compared to control at 1 h postirradiation. Later, radiation-induced -H2AX appearance was reduced at 4 h and almost disappeared within 24 h after irradiation, indicating a time-dependent repair of radiation-induced DSBs. Interestingly, combination treatment with ECL and radiation exhibited significantly higher levels of -H2AX than irradiation alone at the same incubation periods. These results suggest that pretreatment with ECL delays the repair of DSBs induced by radiation and subsequently increases radiosensitivity.

Next we determined the status of the p53-binding protein 1 (53BP1), an important regulator of the cellular response to DSBs that promotes nonhomologous end joining (NHEJ)-mediated DSB repair[18]. As shown in Figure 7, 53BP1 proteins were mainly localized throughout the nucleus of untreated control cells. Treatment with radiation alone markedly induced A549 cells to generate nuclear 53BP1 foci that colocalized with -H2AX foci at DSB sites, presumably to facilitate the repair. Interestingly, pretreatment of ECL prior to irradiation decreased the radiation-induced 53BP1 foci formation in a dose-dependent manner. In contrast, a number of -H2AX foci were additive with cotreatment. Together, ECL could enhance the formation of persistent DSB foci via inhibiting the recruitment of 53BP1 proteins to radiation-induced DSB sites, resulting in the damage repair inhibition.

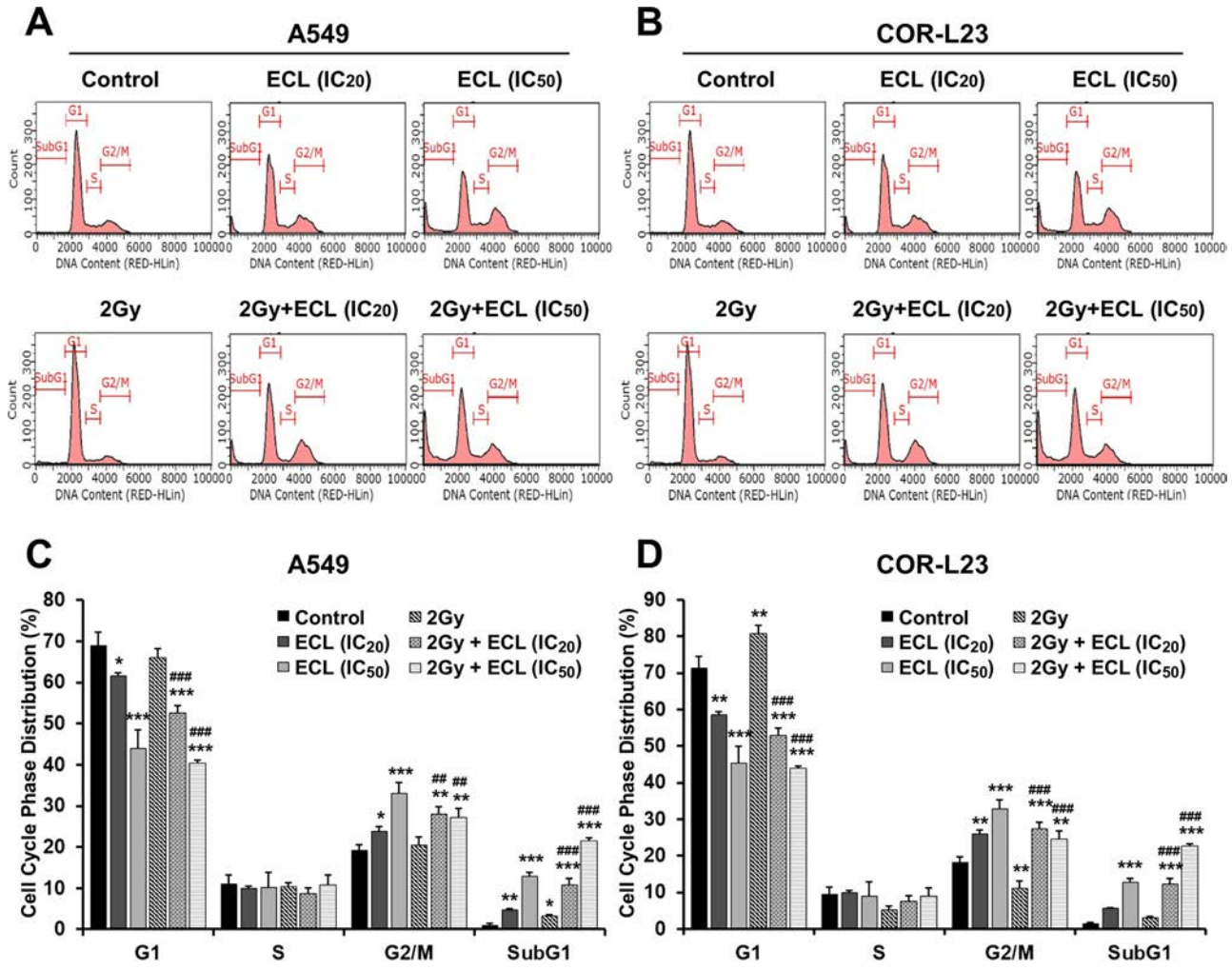

Figure 3. Effects of ECL on cell cycle arrest induction of irradiated non-small cell lung cancer (NSCLC) cells. A549 and COR-L23 cells were treated with ECL for 24 h followed by X-irradiation (2 Gy). Cell cycle was analyzed by flow cytometry, and the representative histograms of cell cycle distribution in A549 (A) and COR-L23 (B) cells are shown. (C, D) The quantitative analysis of the cell cycle phases in A549 and COR-L23 cells, respectively. Data indicated as mean ± SD. $n = 3$. *$p < 0.05$, **$p < 0.01$, ***$p < 0.001$ versus control group. ##$p < 0.01$, ###$p < 0.001$ significant difference when compared with the combination treatment group versus X-irradiation alone.

ECL Inhibited the Repair via Decreasing the Expression of DNA Repair Proteins in X-Irradiated NSCLC Cells

The defective formation of 53BP1 foci prompted us to investigate the expression of lysine-specific demethylase 4 (KDM4D), which promotes 53BP1 foci formation[19] and Ku-80, which is required for the NHEJ repair pathway[20]. As shown in Figure 8, ECL treatment at IC_{50} could significantly suppress the expression of KDM4D but not Ku-80 proteins in A549 and COR-L23 cells. Interestingly, X-ray irradiation alone led to a significant induction of KDM4D and Ku-80 protein expression. Notably, pretreatment with ECL blocked the upregulation of both KDM4D and Ku-80 proteins in irradiated A549 (Fig. 8A–C) and COR-L23 cells (Fig. 8D–F) when compared to irradiation alone. Nevertheless, ECL treatment alone or combined with X-ray did not inhibit the mRNA expression of these molecules (Fig. 8G and H). These data suggest that the combination of X-ray and ECL treatment alters the expression of multiple proteins involved in the DNA repair pathway but does not affect their expression at the transcriptional level.

DISCUSSION

In the present study, we investigated the anticancer and radiosensitization potential of purified ECL, an active natural product from the roots of *E. longifolia* on NSCLC cells. Our initial findings demonstrated that ECL exerts strong and selective cytotoxic effects on A549 and COR-L23 cells, but not on Calu-1, when compared to the normal lung fibroblast WI-38 cells. The differential sensitivity of

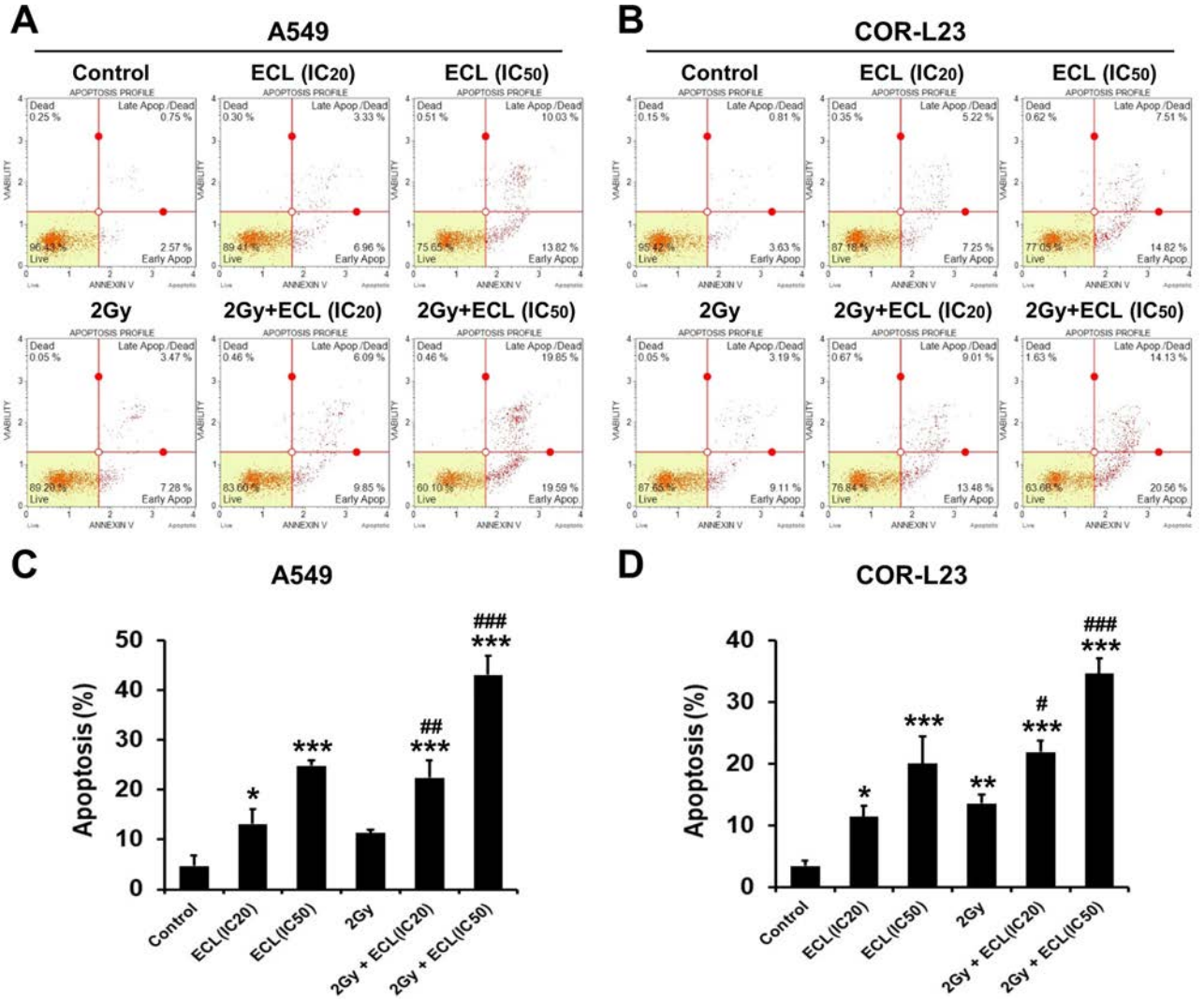

Figure 4. Combinatorial effect of ECL and X-irradiation on the NSCLC cell apoptosis. Cells were preincubated with ECL for 24 h followed by irradiation. The apoptosis was determined by flow cytometry using annexin V/PI staining. Representative dot plots of A549 and COR-L23 cells are shown in (A) and (B), respectively. (C, D) The quantitative analysis of percentage of total apoptotic cells in A549 and COR-L23 cells. Data indicated as mean ± SD. $n = 3$. *$p < 0.05$, **$p < 0.01$, ***$p < 0.001$ versus control. #$p < 0.05$, ##$p < 0.01$, ###$p < 0.001$ versus X-irradiation alone.

these NSCLC cells to ECL might be explained in part by the distinguished population doubling time (DT). Most anticancer agents interfere with cell duplication in some manner, either by damaging DNA, causing cell cycle arrest, or preventing mitosis via stabilizing the cell microtubules. The cells with high proliferation rate are generally more susceptible to these agents than the cells with lower proliferation rate[21]. Therefore, ECL gains the selective cytotoxic effect to both A549 and COR-L23 cells that proliferate (DT, about 20 and 18 h, respectively) more rapidly than WI-38 (DT, about 28 h) and Calu-1 cells (DT, about 37 h). As the value of SI demonstrates the differential activity of a compound, the greater the SI value, the better it was. Moreover, the SI values greater than 3.0 are considered to indicate high selectivity and to be significant as a promising anticancer drug[22]. Therefore, our results indicate that ECL has potential as an anticancer, or chemo-/radiosensitizer agent for rapid proliferating NSCLC cells.

We have demonstrated for the first time that ECL enhances the radiosensitivity of A549 and COR-L23 NSCLC cells to X-radiation in vitro. ECL is a potent radiosensitizer since the noncytotoxic concentration exhibited the nearby radiation enhancement ratio with its cytotoxic concentration when combined with low radiation doses (1, 2, and 3 Gy). Our results suggest that a noncytotoxic dose of ECL might be sufficient for therapeutic application as a clinical radiosensitizer because the typical curative

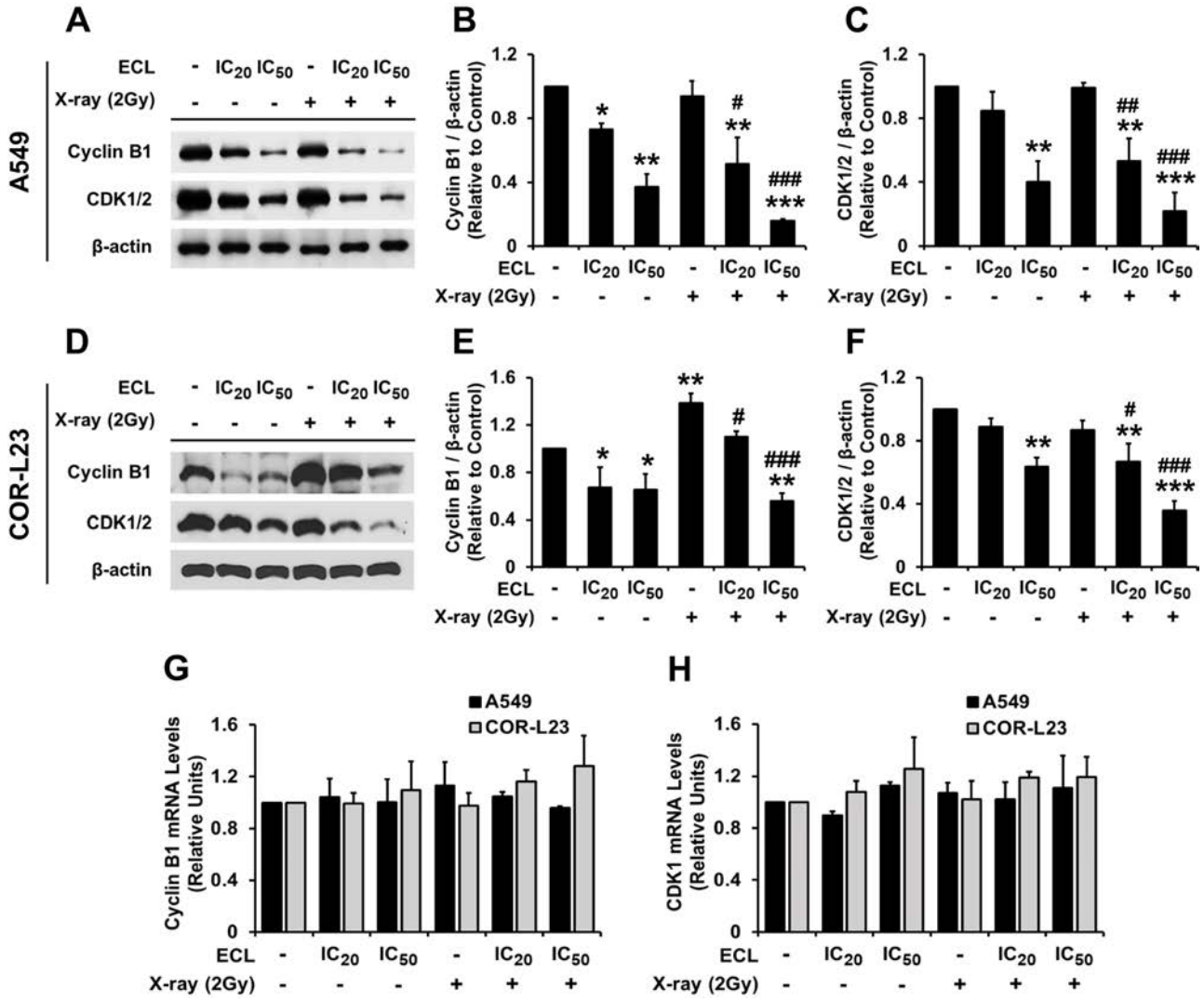

Figure 5. Effects of ECL on the expression of G_2/M regulatory proteins cyclin B1 and cyclin-dependent kinase 1/2 (CDK1/2). The representative immunoblots of cyclin B1 and CDK1/2 proteins in A549 (A) and COR-L23 (D) cells treated with ECL or X-ray or in combination. Semiquantitative analyses of cyclin B1 (B, E) and CDK1 (C, F) are shown in both A549 and COR-L23 cells. The mRNA levels of cyclin B1 (G) and CDK1 (H) in both NSCLC cells were analyzed by reverse transcription-quantitative polymerase chain reaction (RT-qPCR). Data are shown as the mean ± SD. $n = 3$. *$p < 0.05$, **$p < 0.01$, ***$p < 0.001$ versus control group. #$p < 0.05$, ##$p < 0.01$, ###$p < 0.001$ significantly different when compared with the combination treatment group versus X-irradiation alone.

dose for a solid epithelial tumor including NSCLC ranges from 60 to 80 Gy in 1.8–2 Gy fractions[23].

Our studies on the molecular mechanisms of ECL in antiproliferation revealed that ECL itself delays the rate of NSCLC cell proliferation by inducing G_2/M cell cycle arrest. It is well known that cancer cells are most sensitive to ionizing radiation during G_2/M, less sensitive during G_1, and least sensitive in S phase[5]. As radiosensitizer, various natural agents such as genistein and gingerol have been reported to improve radiosensitivity of several cancer cell types by blocking them at G_2/M phase[8,9]. The combined treatment of radiation and ECL obviously augmented the number of cells at the G_2/M phase and sharply increased the number of cells at sub-G_1 phase, committing the cells to apoptosis compared to X-irradiation alone. Cell commitment to either remains in the G_2/M or progress through G_2 into mitosis requires the activation of CDK1–cyclin B1 complex at the beginning of mitosis. Decreased cyclin B1 and CDK1 protein expression and its kinase activity contribute to G_2/M arrest[24]. Herein, ECL combined with radiation downregulated the expression of cyclin B1 and CDK1/2 proteins more effectively than the single X-ray treatment. Therefore, ECL positioned more cells in the radiosensitive G_2/M phase at the time of radiation and enhanced the radiation-induced cell killing. It is noteworthy that cell cycle arrest functions to allow extra time for

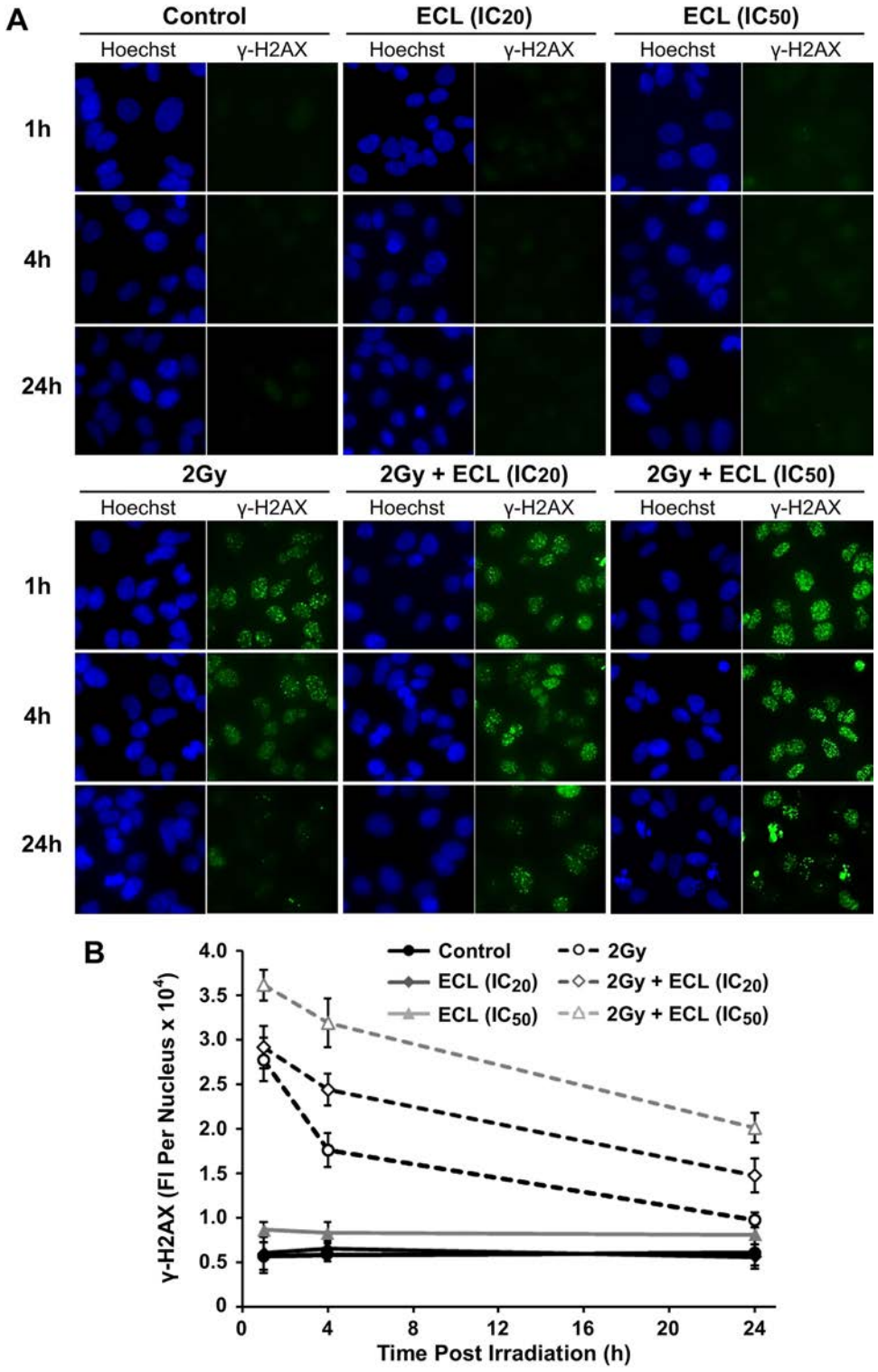

Figure 6. Effect of ECL on radiation-induced -H2AX expression. A549 cells were pretreated with ECL for 24 h followed by X-irradiation (2 Gy). The cells were fixed at 1, 4, and 24 h postirradiation, then immunofluorescence staining was performed. (A) The representative images of -H2AX foci. (B) The total average fluorescence intensities of -H2AX per nucleus were analyzed by ImageJ software. Each point represents an average data of 995 cells. Data are expressed as mean ± SD. $n = 3$.

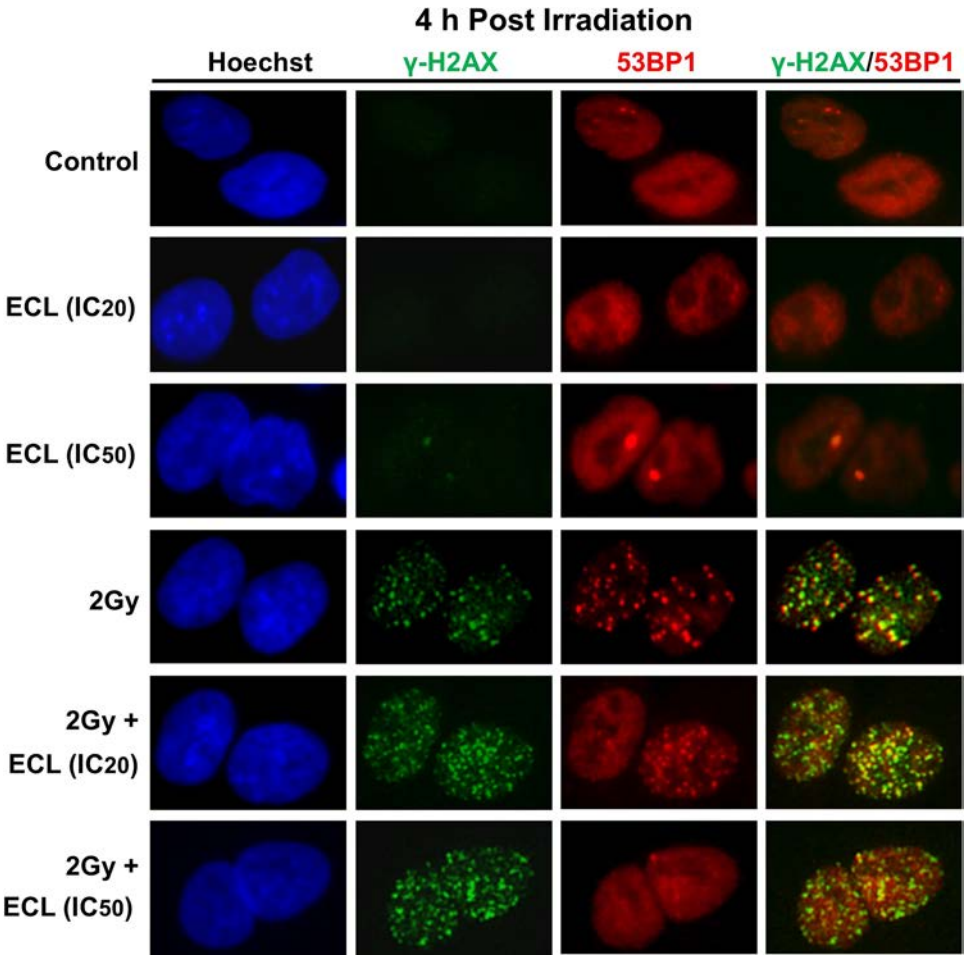

Figure 7. Effect of ECL on 53BP1 foci formation in radiation-treated A549 cells. The cells were pretreated with ECL for 24 h, irradiated (2 Gy), then grown for 4 h before performing the immunofluorescence staining. Representative immunofluorescence images of A549 cells stained for -H2AX and 53BP1 foci at 4 h postirradiation are shown.

repairing DNA damage. Once the level of damage is irreparable, cells either remain permanently arrested (senescence) or undergo programmed cell death[25]. Thus, ECL might enhance the radiation effect on NSCLC cell killing by altering the DNA damage response and repair systems.

Ionizing radiation-induced DSBs followed by cell death are recognized as the main mechanism for cancer cell elimination by radiotherapy, and it is often used to predict the radiosensitivity of tumor cells[4]. Additionally, an increase in DSBs and an impaired DSB repair system are related to the efficacy of potential radiosensitizers[6,7]. It is well established that DSBs are associated with recruitment of -H2AX, which is well known as an indicator of DSBs and a marker for DSB repair kinetics[26]. We observed that the expression of -H2AX was significantly enhanced following the combined treatment of X-rays and ECL when compared to X-rays treated alone. Thus, the repair of radiation-induced DSB was likely attenuated by the cotreatment, resulting in the persistence of cell damage. NHEJ is one of two well-known mechanisms for the repair of DSBs, which is an error-prone process and active throughout the cell cycle. The key proteins in the NHEJ process are composed of DNA-dependent protein kinase (DNA-PKcs) and Ku (Ku-70/-80)[20]. The 53BP1 plays a major role in facilitating DSB repair by the NHEJ pathway[18]. Our result revealed that ECL treatment blocks the recruitment of 53BP1 to the radiation-induced DSB sites. Inhibition of 53BP1 foci formation has impaired the NHEJ integrity of DSB[27]. Downregulation of 53BP1 by sh-RNA is known to enhance radiosensitivity in cancer cells[28]. Moreover, 53BP1-deficient mice were growth retarded, immune deficient, and radiation sensitive[29]. Therefore, the inefficient formation of radiation-induced 53BP1 foci caused by ECL may downregulate the NHEJ repair and could lead to elevated sensitivity to radiation.

As previously reported, cells lacking Ku were defective in DSB rejoining and were highly sensitive to ionizing radiation[30]. In addition, overexpression of Ku-70/Ku-80

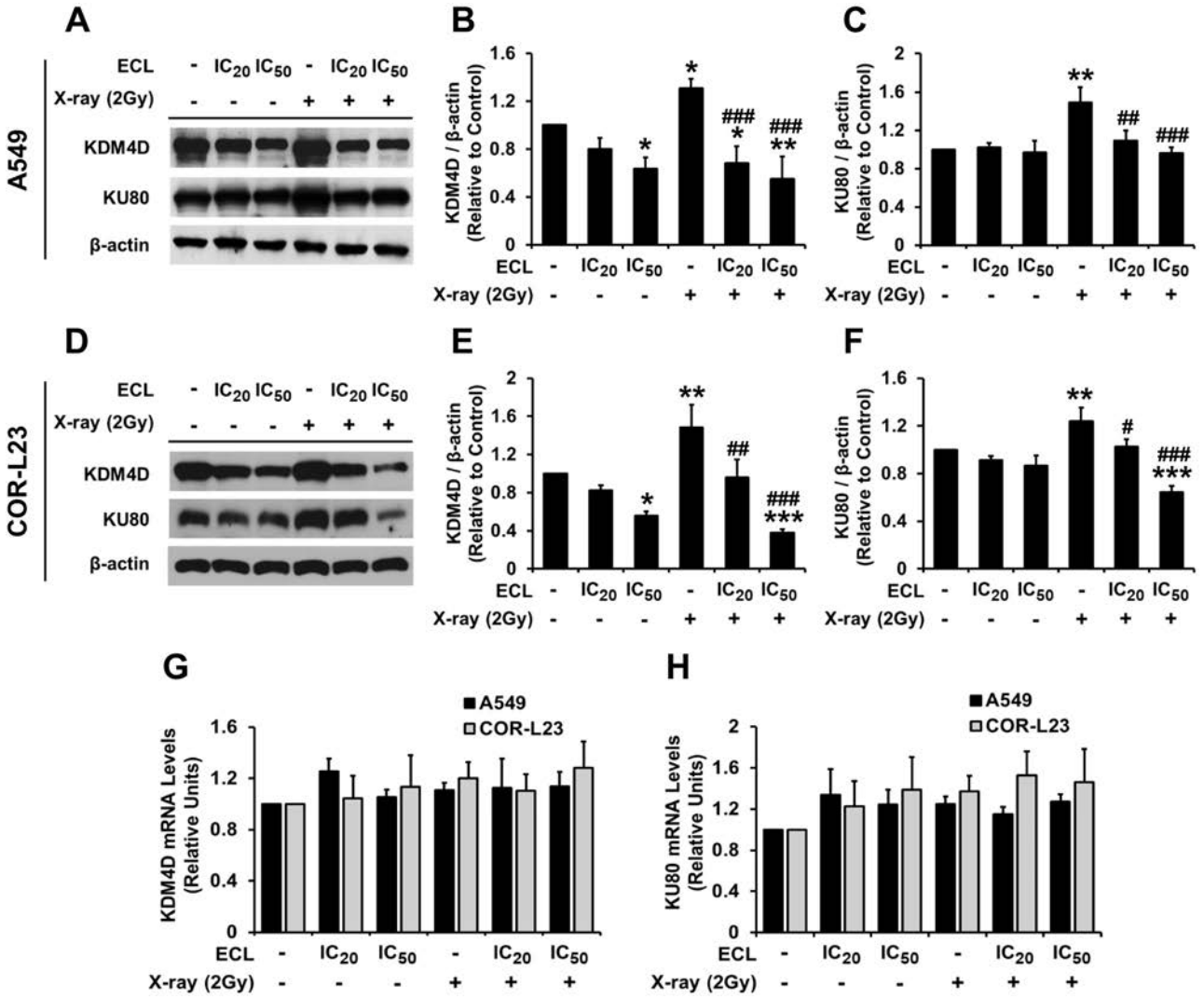

Figure 8. Effects of ECL on the expression of DNA repair proteins KDM4D and Ku-80. The representative immunoblots of KDM4D and Ku-80 proteins in A549 (A) and COR-L23 (D) cells treated with ECL or X-ray or in combination. Semiquantitative analyses of KDM4D (B, E) and Ku-80 (C, F) are shown in both A549 and COR-L23 cells. The mRNA levels of KDM4D (G) and Ku-80 (H) in both NSCLC cells were analyzed by RT-qPCR. The data are shown as the mean ± SD. $n = 3$. *$p < 0.05$, **$p < 0.01$, ***$p < 0.001$ versus control group. #$p < 0.05$, ##$p < 0.01$, ###$p < 0.001$ significantly different when compared with the combination treatment group versus X-irradiation alone.

has been correlated with radioresistance in cervical, breast, and bladder cancers[31]. ECL pretreatment could interfere with the NHEJ repair pathway by decreasing the radiation-induced Ku-80 expression. Nonetheless, several proteins are also required to promote the recruitment of 53BP1 to DSB sites as well as KDM4D. The knockdown of KDM4D disrupted the damage-induced 53BP1 foci formation and sensitized cells to radiation-induced DNA damage[19]. Our results indicate that X-rays induced while the ECL pretreatment downregulated the KDM4D protein expression in the NSCLC cells. These could result in the ineffective 53BP1 foci formation and defective NHEJ repair. Therefore, the radiosensitizing effect of ECL is also likely associated with ablation in the efficacy of NHEJ repair pathways in the irradiated NSCLC cells whose cell cycle becomes arrested during G_2/M phase followed by the induction of apoptosis-related death.

ECL downregulated the expression of G_2/M regulatory proteins (cyclin B1, CDK1) and DNA repair proteins (KDM4D and Ku-80) in NSCLC by a mechanism at the posttranscriptional level. In our study, ECL did not alter the level of these mRNAs while it significantly decreased their protein, suggesting that ECL does not interfere with the transcription of these genes. As previously reported in HUVEC endothelial cells, ECL acts as an inhibitor of

proteins' synthesis[32]. Moreover, quassinoids have been previously shown to inhibit the peptide bond formation by binding to ribosomal peptidyl transferase in eukaryotic cells[33]. Thus, ECL also likely inhibits protein synthesis and/or maybe other posttranscriptional processes in human NSCLC cells.

In summary, ECL has selective cytotoxic activity toward A549 and COR-L23 NSCLC cells compared to noncancerous cells. Pretreatment with ECL followed by X-rays effectively induces in vitro radiosensitization in both NSCLC cells. Our study suggests that ECL likely exerts radiosensitizing activity through multiple mechanisms: 1) redirection of NSCLC cells into the radiosensitive G_2/M phase of the cell cycle, 2) delay irradiation-induced DNA damage repair pathways, and 3) induction of apoptosis. Thus, ECL may offer an alternative treatment strategy in combination with conventional radiotherapy for enhancing the efficacy of X-ray irradiation against human NSCLC.

ACKNOWLEDGMENTS: This research work was funded by the Royal Golden Jubilee Ph.D. (RGJ-PHD) Programme, Thailand Research Fund (TRF) (Grant No. PHD/0088/2558), the Faculty of Medicine Research Fund, Faculty of Medicine, Chiang Mai University, Chiang Mai, Thailand (Grant No. 090-2560). Moreover, the authors wish to acknowledge the National Institute of Radiological Sciences (NIRS), Chiba, Japan, and the Faculty of Medicine, Chiang Mai University, Chiang Mai, Thailand, for providing research facilities and support. The authors would like to thank the Nuclear Researchers Exchange Program FY2017 of the Ministry of Education, Culture, Sports, Science and Technology (MEXT), Government of Japan, for financially supporting Ms. Dukaew in Japan. In addition, we would like to thank Professor Arthur L. Haas, Health Sciences Center School of Medicine, Louisiana State University, for critical reading of the manuscript and useful comments. The authors declare no conflicts of interest.

REFERENCES

1. Bray F, Ferlay J, Soerjomataram I, Siegel RL, Torre LA, Jemal A. Global cancer statistics 2018: GLOBOCAN estimates of incidence and mortality worldwide for 36 cancers in 185 countries. CA Cancer J Clin. 2018;68(6):394–424.
2. Zappa C, Mousa SA. Non-small cell lung cancer: Current treatment and future advances. Transl Lung Cancer Res. 2016;5(3):288–300.
3. Glide-Hurst CK, Chetty IJ. Improving radiotherapy planning, delivery accuracy, and normal tissue sparing using cutting edge technologies. J Thorac Dis. 2014;6(4):303–18.
4. Mladenov E, Magin S, Soni A, Iliakis G. DNA double-strand break repair as determinant of cellular radiosensitivity to killing and target in radiation therapy. Front Oncol. 2013;3:113.
5. Pawlik TM, Keyomarsi K. Role of cell cycle in mediating sensitivity to radiotherapy. Int J Radiat Oncol Biol Phys. 2004;59(4):928–42.
6. Mu F, Liu T, Zheng H, Xie X, Lei T, He X, Du S, Tong R, Wang Y. Mangiferin induces radiosensitization in glioblastoma cells by inhibiting nonhomologous end joining. Oncol Rep. 2018;40(6):3663–73.
7. Liu XX, Sun C, Jin XD, Li P, Zheng XG, Zhao T, Li Q. Genistein sensitizes sarcoma cells in vitro and in vivo by enhancing apoptosis and by inhibiting DSB repair pathways. J Radiat Res. 2016;57(3):227–37.
8. Liu X, Sun C, Jin X, Li P, Ye F, Zhao T, Gong L, Li Q. Genistein enhances the radiosensitivity of breast cancer cells via G(2)/M cell cycle arrest and apoptosis. Molecules 2013;18(11):13200–17.
9. Luo Y, Chen X, Luo L, Zhang Q, Gao C, Zhuang X, Yuan S, Qiao T. [6]-Gingerol enhances the radiosensitivity of gastric cancer via G2/M phase arrest and apoptosis induction. Oncol Rep. 2018;39(5):2252–60.
10. Rehman SU, Choe K, Yoo HH. Review on a traditional herbal medicine, Eurycoma longifolia Jack (Tongkat Ali): Its traditional uses, chemistry, evidence-based pharmacology and toxicology. Molecules 2016;21(3):331.
11. Thu HE, Hussain Z, Mohamed IN, Shuid AN. Eurycoma longifolia, a potential phytomedicine for the treatment of cancer: Evidence of p53-mediated apoptosis in cancerous cells. Curr Drug Targets 2018;19(10):1109–26.
12. Miyake K, Li F, Tezuka Y, Awale S, Kadota S. Cytotoxic activity of quassinoids from Eurycoma longifolia. Nat Prod Commun. 2010;5(7):1009–12.
13. Kuo PC, Damu AG, Lee KH, Wu TS. Cytotoxic and antimalarial constituents from the roots of Eurycoma longifolia. Bioorg Med Chem. 2004;12(3):537–44.
14. Phannasorn W, Khanaree C, Wongnoppavich A, Chewonarin T. The effect of purple rice (Oryza sativa L. indica) extract on the inflammatory response in a colon cancer cell line and dextran sulfate-induced tumor promotion in the rat colon. Mol Cell Toxicol. 2017;13(4):433–42.
15. Kobayashi A, Tengku Ahmad TAF, Autsavapromporn N, Oikawa M, Homma-Takeda S, Furusawa Y, Wang J, Konishi T. Enhanced DNA double-strand break repair of microbeam targeted A549 lung carcinoma cells by adjacent WI38 normal lung fibroblast cells via bi-directional signaling. Mutat Res. 2017;803–805:1–8.
16. Wongnoppavich A, Dukaew N, Choonate S, Chairatvit K. Upregulation of maspin expression in human cervical carcinoma cells by transforming growth factor beta1 through the convergence of Smad and non-Smad signaling pathways. Oncol Lett. 2017;13(5):3646–52.
17. Chang L, Graham P, Hao J, Ni J, Deng J, Bucci J, Malouf D, Gillatt D, Li Y. Cancer stem cells and signaling pathways in radioresistance. Oncotarget 2016;7(10):11002–17.
18. Panier S, Boulton SJ. Double-strand break repair: 53BP1 comes into focus. Nat Rev Mol Cell Biol. 2014;15(1):7–18.
19. Khoury-Haddad H, Guttmann-Raviv N, Ipenberg I, Huggins D, Jeyasekharan AD, Ayoub N. PARP1-dependent recruitment of KDM4D histone demethylase to DNA damage sites promotes double-strand break repair. Proc Natl Acad Sci USA 2014;111(7):E728–37.
20. Mao Z, Bozzella M, Seluanov A, Gorbunova V. DNA repair by nonhomologous end joining and homologous recombination during cell cycle in human cells. Cell Cycle 2008;7(18):2902–6.
21. Mitchison TJ. The proliferation rate paradox in antimitotic chemotherapy. Mol Biol Cell 2012;23(1):1–6.
22. Duangprompo W, Aree K, Itharat A, Hansakul P. Effects of 5,6-dihydroxy-2,4-dimethoxy-9,10-dihydrophenanthrene on G2/M cell cycle arrest and apoptosis in human lung carcinoma cells. Am J Chin Med. 2016;44(7):1473–90.
23. Wistuba II, Brambilla E, Noguchi M. Classic anatomic pathology and lung cancer. In: Ball D, Scagliotti GV, editors.

IASLC thoracic oncology, 2nd edition. Philadelphia, PA: Elsevier, 2018. p. 143–63.
24. Otto T, Sicinski P. Cell cycle proteins as promising targets in cancer therapy. Nat Rev Cancer 2017;17:93.
25. Ciccia A, Elledge SJ. The DNA damage response: Making it safe to play with knives. Mol Cell 2010;40(2):179–204.
26. Sharma A, Singh K, Almasan A. Histone H2AX phosphorylation: A marker for DNA damage. Methods Mol Biol. 2012;920:613–26.
27. Dimitrova N, Chen YC, Spector DL, de Lange T. 53BP1 promotes non-homologous end joining of telomeres by increasing chromatin mobility. Nature 2008;456(7221):524–8.
28. Gou Q, Xie Y, Liu L, Xie K, Wu Y, Wang Q, Wang Z, Li P. Downregulation of MDC1 and 53BP1 by short hairpin RNA enhances radiosensitivity in laryngeal carcinoma cells. Oncol Rep. 2015;34(1):251–7.
29. Ward IM, Minn K, van Deursen J, Chen J. p53 Binding protein 53BP1 is required for DNA damage responses and tumor suppression in mice. Mol Cell Biol. 2003;23(7): 2556–63.
30. Mahaney BL, Meek K, Lees-Miller SP. Repair of ionizing radiation-induced DNA double-strand breaks by non-homologous end-joining. Biochem J. 2009;417(3):639–50.
31. Pucci S, Mazzarelli P, Rabitti C, Giai M, Gallucci M, Flammia G, Alcini A, Altomare V, Fazio VM. Tumor specific modulation of KU70/80 DNA binding activity in breast and bladder human tumor biopsies. Oncogene 2001;20(6):739–47.
32. Malainer C, Schachner D, Sangiovanni E, Atanasov AG, Schwaiger S, Stuppner H, Heiss EH, Dirsch VM. Eurycomalactone inhibits expression of endothelial adhesion molecules at a post-transcriptional level. J Nat Prod. 2017;80(12):3186–93.
33. Guo Z, Vangapandu S, Sindelar RW, Walker LA, Sindelar RD. Biologically active quassinoids and their chemistry: Potential leads for drug design. Curr Med Chem. 2005;12(2):173–90.